Use of Advanced Neutron Optics in a Liquids Reflectometer

John F. Ankner
Spallation Neutron Source Project
Oak Ridge National Laboratory

[Poster presented at 6SXNS Conference
at Noordwijkerhout, The Netherlands
16 September 1999]

SNS Document IS-1.1.8.2-6021-RE-A-00

Use of Advanced Neutron Optics in a Liquids Reflectometer

John F. Ankner
Spallation Neutron Source, Oak Ridge National Laboratory

Introduction

Reflectivity measurements are most often performed by varying the angle of incidence of a monochromatic neutron or x-ray beam onto the surface of a sample and measuring the reflected intensity. Since neutron energy is proportional to the square of velocity, if one can define a particular origin in time for the radiation, the wavelength can be determined by time-of-flight,

$$E = \frac{1}{2} m_n v^2 = \frac{h^2}{2 m_n l^2} \Rightarrow l = \frac{h}{m_n} \frac{t_{\mathrm{MD}}}{l_{\mathrm{MD}}},$$

where t_{MD} is the source-detector time-of-flight and l_{MD} the distance. At a reactor, the time origin can be defined by means of a chopper; at a pulsed spallation source, the time origin is intrinsic, coinciding roughly with the time of impact of a proton beam on a heavy-metal target. By utilizing such a time-stamped beam, one can measure reflectivity at a fixed angle of incidence by collecting intensity as a function of l .

Time-of-flight reflectometry possesses advantages relative to the fixed-wavelength method. Collecting data simultaneously over a range of wavelengths is more efficient and in principle eliminates the need for complicated and expensive angular positioning. The range of Q accessible at a single angular setting depends explicitly on the wavelengths available. In practice, however, source repetition rate limits the wavelength bandwidth,

$$l_{\max} - l_{\min} = \frac{h}{m_n} \frac{1}{l_{\mathrm{MD}}} \frac{1}{f_{\mathrm{M}}}$$

where f_{M} is the source frequency (e.g. 50 Hz at ISIS). Every $1/f_{\mathrm{M}}$, a new batch of neutrons arrives with a different time-stamp. One increases bandwidth by constructing as short an instrument as possible (small l_{MD}) and sometimes by employing choppers to reject pulses. Pulse rejection eliminates all neutrons from adjacent pulses and so reduces incident flux. In addition, increasing the bandwidth eventually exposes one to low-intensity regions of the neutron moderator Maxwell distribution, further decreasing flux. For these reasons, except in instances where data must be collected at a single angular setting, one utilizes the available bandwidth and measures at several different incident angles (typically 3 at the 30-Hz IPNS POSY-II instrument with $2.5\ \text{Å} < l < 15\ \text{Å}$).

Designing a reflectometer to study liquid surfaces poses difficult challenges. Since the sample cannot be tilted, one must move the incident beam (accomplished by tipping the monochromator on fixed-wavelength instruments) or utilize a broad wavelength bandwidth in a fixed beam. A third alternative employs several incident beams and a modest wavelength bandwidth , a hybrid approach that combines efficient broadband data collection with the capability to vary the angle of the incident beam. We have adopted this approach in our conceptual design of a liquids reflectometer for the Spallation Neutron Source (SNS), a 60 Hz, 2 MW scattering facility under construction at the Oak Ridge National Laboratory.

Acceptance Diagrams: Monte Carlo for the Impatient

We have employed an acceptance-diagram formalism to evaluate the performance of optical components[1,2]. The method is essentially similar to Monte Carlo modeling, but treats neutron populations in phase space, and thus provides a conceptual framework along with quantitative flux determination. Consider an aperture viewing a planar neutron source that emits uniformly at all angles.

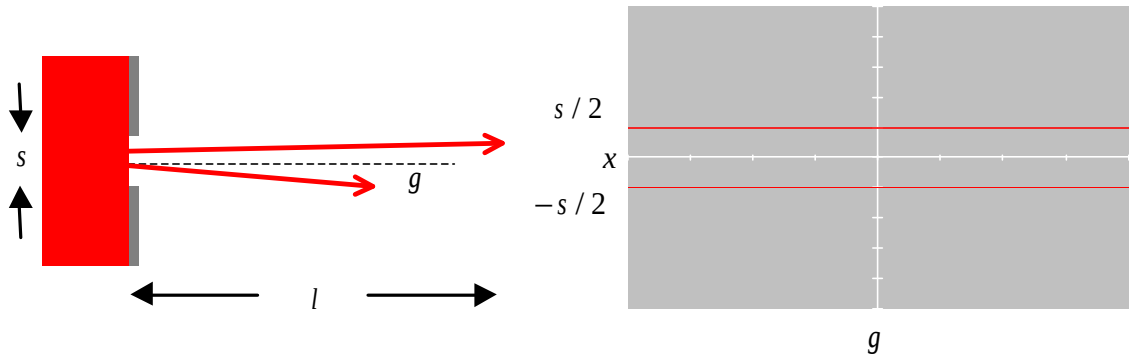

The plot on the right shows the neutron spatial coordinate at the source plotted against the angular divergence g. Since all values of g are present, the area between the red lines describes the source population at the aperture ($-s/2 < x < s/2$).

If the neutrons do not encounter an obstruction, their spatial and angular coordinates transform as follows:

$$x^* = x + l \tan g$$

$$g^* = g.$$

On the acceptance diagram, points with positive angular divergence move up and those with negative divergence move down.

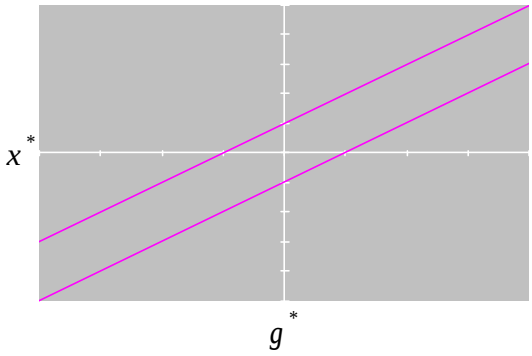

The magenta lines enclose this freely translating population of neutrons. Placing absorbing walls out to a distance l collimates the beam and so limits the phase-space volume.

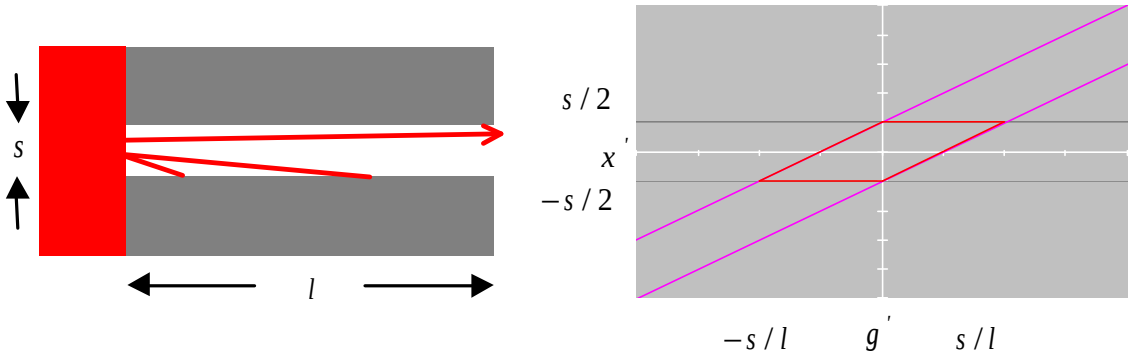

Any neutrons with position and divergence coordinates outside the red parallelogram are not transmitted. The area enclosed by the parallelogram defines the phase space available to neutrons at the collimator exit. If one coats the collimator walls with reflecting material, more flux can be transmitted. For thermal and cold neutrons, the critical angle for total external reflection $g_c \sim l$. Any neutrons that strike the guide wall at $g < g_c$ will be reflected. These reflections can be represented geometrically in the acceptance diagram.

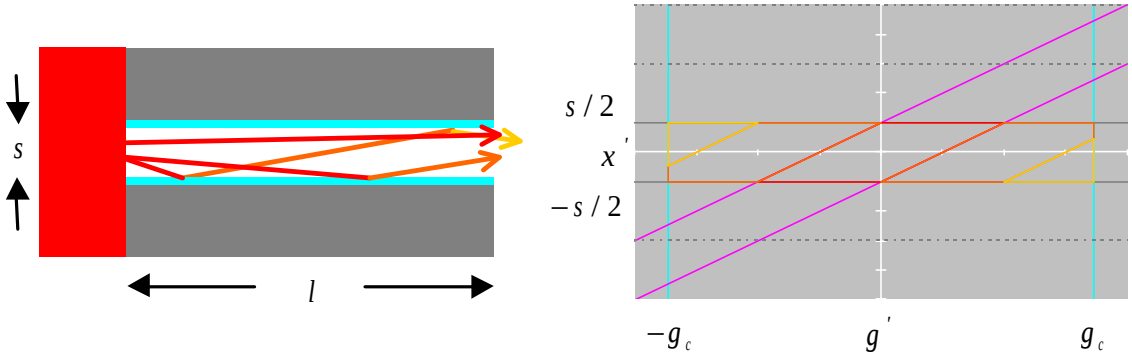

Reflection m times by the guide is described by transformation of the polygon vertices[3].

$$x' = (-1)^m (x + l \tan g - ms)$$

$$g' = (-1)^m (g + 2mg^{\text{taper}})$$

$$|g'| < g_c + g^{\text{taper}},$$

where $g^{\text{taper}} = 0$ for a parallel-sided guide. The next downstream optical component receives as input this acceptance. One can model quite sophisticated components using these basic principles, as we show below.

Neutron Source

Neutrons at the SNS will be produced by spallation from a Hg target struck by 1 GeV protons. The highly energetic neutrons created by this process will be slowed by several different moderators. The liquids reflectometer will view a super-critical H_2 moderator at 20 K.

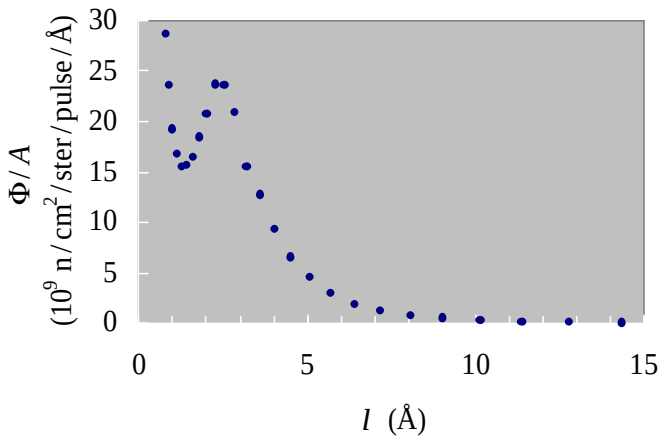

Peak flux Φ in this $A = 10 \times 12\ \mathrm{cm}^2$ moderator occurs at 2.5 Å, with a tail extending to long wavelengths[4]. To preserve the time structure of the neutron pulse, the source is undermoderated: high-energy neutrons remain in the beam (note the steep tail for $l < 1$ Å). Preventing these energetic neutrons from reaching the detector is a primary design concern. The emission time uncertainty of the neutrons emerging from the moderator limits the Q resolution of the instrument:

$$3\ \text{Å} < l < 15\ \text{Å} \Rightarrow 50\ m\text{sec} < dt < 200\ m\text{sec}.$$

Microguide Bender

The prompt pulse of highly energetic neutrons can damage detectors. These neutrons also scatter from steel shielding or a concrete floor and make their way to the detector as background. So, one would like to dispose of them as close to the point of production as possible. A t_0 chopper consists of a slug of Ni alloy that rotates at the source frequency and scatters the prompt neutrons into surrounding shielding. However, due to mechanical constraints, the chopper cannot be placed closer than 5 m from the moderator and the alloy slug cannot be thicker than about 30 cm. We have therefore investigated using a microguide bending device as a high-pass wavelength filter.

Microguides are essentially collimators with mirror-coated blades. These devices transmit more intensity and angular divergence than single-channel guides of equivalent collimating power. We can insert neutron guide in the beam shutter located 2.5 m from the moderator. If we employ 4 50-cm-long $10 \times 12\ \mathrm{cm}^2$ segments in the 2-m-long shutter, each offset 11 mradian with respect to the previous component, we eliminate direct line-of-sight 2 m before the beam exits the downstream tapered guide. The exit acceptance diagram for 9-Å neutrons and five-channel microguide elements with $4g_c^{\mathrm{Ni}}$ supermirror guide coatings exhibits a rich menagerie of reflections.

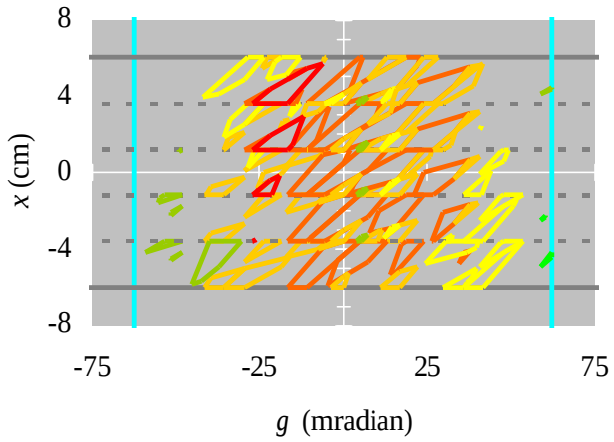

The polygons are color-coded by number of reflections m (0-red, 1-orange, 2-gold, 3-yellow, 4-lime, 5-green). The acceptance of the device increases with the number of blades n, saturating above 5.

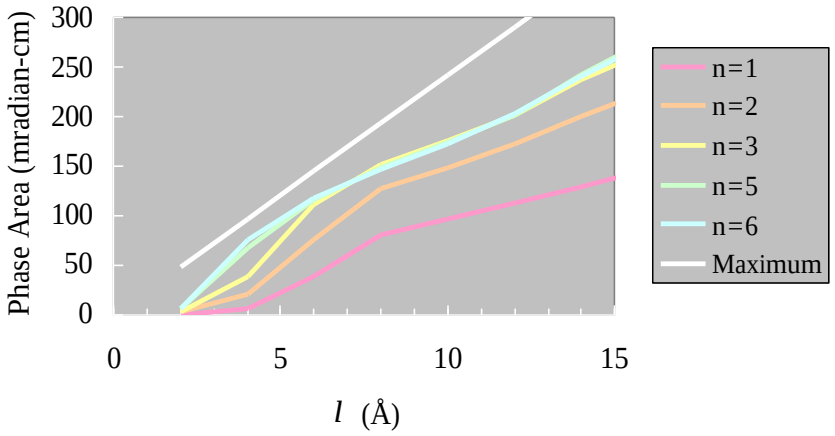

Phase area is the summed area of the polygons in the acceptance diagram. Since the microguide bender eliminates line-of-sight neutrons, the maximum phase area is $2g_c s$, corresponding to a situation in which neutrons of all angular divergences less than the critical angle are accepted over the entire exit aperture width. Performing a similar analysis in the other guide dimension and multiplying the phase areas yields acceptance X in units of steradian-cm^2 that one can multiply by the source flux Φ to calculate instrument count rates (see below).

Tapered Guide

After passing through the microguide bender, the neutrons enter a $4g_c^{Ni}$-coated, 6-m-long guide that tapers from 12 to 1.75 cm. The tapered guide increases the divergence provided by the microguide and creates the angular "bandwidth" sampled during measurement of the fixed liquid surface.

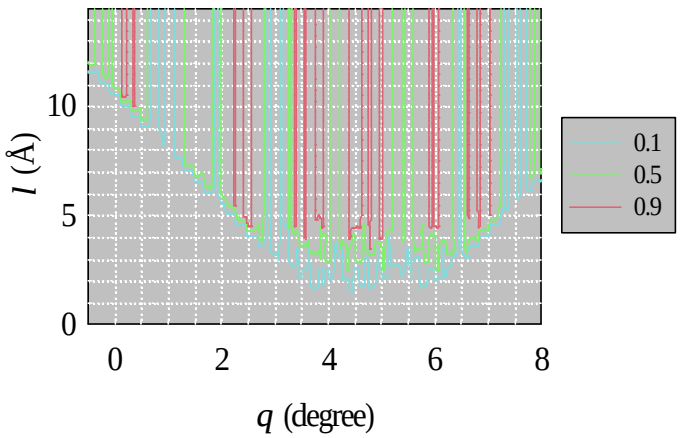

Each reflection from the wall of the tapered guide increases divergence by $2g^{\text{taper}}$. The contour plot shows acceptance area fraction (10, 50, and 90% of $2g_c s$) as a function of λ and exit angle θ. The centroid of the tapered guide is inclined 4.75° from the horizontal. By placing variable-aperture slits (1 m separation) at the guide exit, we can sample this distribution.

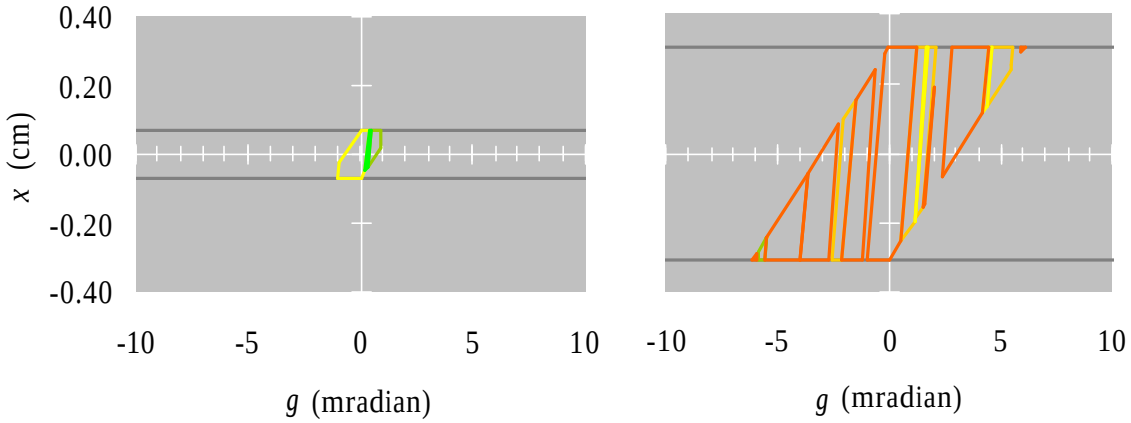

The diagram on the left shows the acceptance of 0.14 cm slits viewing at $\theta = 2.06^\circ$, while the right shows 0.61 cm slits at $\theta = 4.75^\circ$ (in both cases $\lambda = 9$ Å). The narrow aperture accepts 0.89 of the phase area of a slit viewing an infinite-divergence source, while the wide aperture accepts 0.86. However, neutrons passing through the narrow aperture view the tapered guide off its centerline and, on average, undergo more reflections in the guide optics: 3.33 vs. 1.27 for the wide aperture. Assuming an average reflectivity of 0.9 for the $4g_c^{\text{Ni}}$ guide coatings, the neutron count rates are actually reduced by factors of $0.70 \times 0.89 = 0.62$ (narrow) and $0.87 \times 0.86 = 0.75$ (wide) from the theoretical maxima.

Controlling the time-stamp of the neutrons entering the detector is vital to the operation of time-of-flight instruments. The SNS will run at 60 Hz, so every 16.7 msec, the target sends out a new batch of neutrons. Three bandwidth choppers, operating at 60 Hz, located 5.30, 7.30, and 9.75 m from the moderator will be phased to pass wavelength bands of 0.5-5 Å (first frame), 5.5-10 Å (second frame), or 10.5-15 Å (third frame) cleanly through the optical system.

Simulated Data

Having calculated the acceptance of the optics and knowing the source flux, we can estimate count rates for actual samples. Incident counts/sec in a given wavelength band $d\lambda$ are given by

$$I(\lambda, q, t) = \frac{f_M}{A} \Phi(\lambda, t) r^{\bar{m}} d\lambda,$$

where $f_M = 60$ pulse/sec, $A = 120$ cm^2, Φ is the moderator flux plotted above, X is the product of vertical (X_v discussed above) and horizontal (X_h) acceptance areas, r is the average reflectivity of the guide coatings (use 0.9 below), m the average number of bounces in the guides, and $d\lambda$ is the wavelength uncertainty (use $d\lambda / \lambda = 0.05$). The horizontal guide tapers from 10 to 3 cm over the same 6-m length as the vertical and then is collimated by 3-cm slits before the sample. We have set up a spreadsheet to calculate I based on these parameters, an example of which ($q = 7^\circ$) is shown below.

q =	7.00									
λ	$f\Phi/A$	Xh	Xv	$m$avg	$\Delta\lambda$	r^$m$avg	$I(t)$	Q	R	$RI(t)$
(Å)	(n/cm2/ster/sec/Å)	(cm-radian)	(cm-radian)		(Å)		(n/sec)	(Å-1)		(n/sec)
1.50	9.552E+11	0.000E+00	3.044E-02	0.00	0.08	1.00	0.00E+00	1.0210		
2.00	1.229E+12	0.000E+00	3.044E-02	0.00	0.10	1.00	0.00E+00	0.7657		
2.50	1.415E+12	0.000E+00	3.044E-02	4.18	0.13	0.64	0.00E+00	0.6126		
3.00	1.126E+12	2.700E-05	3.044E-02	4.18	0.15	0.64	8.94E+04	0.5105		
3.50	8.064E+11	8.750E-04	3.044E-02	3.74	0.18	0.67	2.53E+06	0.4376	7.65E-08	0.19
4.00	5.802E+11	3.209E-03	3.044E-02	4.22	0.20	0.64	7.27E+06	0.3829	7.24E-08	0.53
4.50	4.026E+11	7.113E-03	3.044E-02	4.42	0.23	0.63	1.23E+07	0.3403	2.40E-08	0.30
5.00	2.910E+11	1.098E-02	3.044E-02	4.50	0.25	0.62	1.51E+07	0.3063	9.71E-09	0.15
5.50	2.130E+11	1.162E-02	3.044E-02	4.50	0.28	0.62	1.29E+07	0.2784	1.20E-07	1.55
6.00	1.542E+11	1.179E-02	3.044E-02	4.53	0.30	0.62	1.03E+07	0.2552	4.24E-07	4.37
6.50	1.086E+11	1.179E-02	3.044E-02	4.53	0.33	0.62	7.86E+06	0.2356	9.88E-07	7.76
7.00	8.220E+10	1.179E-02	3.044E-02	4.53	0.35	0.62	6.40E+06	0.2188	1.80E-06	11.53
7.50	6.540E+10	1.179E-02	3.044E-02	4.53	0.38	0.62	5.46E+06	0.2042	2.89E-06	15.78
8.00	5.064E+10	1.179E-02	3.044E-02	4.53	0.40	0.62	4.51E+06	0.1914	4.30E-06	19.39
8.50	4.218E+10	1.179E-02	3.044E-02	4.53	0.43	0.62	3.99E+06	0.1802	5.92E-06	23.62
9.00	3.432E+10	1.179E-02	3.044E-02	4.53	0.45	0.62	3.44E+06	0.1702	7.83E-06	26.92
9.50	2.892E+10	1.179E-02	3.044E-02	4.53	0.48	0.62	3.06E+06	0.1612	1.00E-05	30.58
10.00	2.382E+10	1.179E-02	3.044E-02	4.53	0.50	0.62	2.65E+06	0.1531	1.24E-05	32.87

For the count-rate calculation, we have used a 20-Å-thick layer of scattering density $b/V = 2\times10^{-6}$ Å^{-2} atop protonated water. Each interface exhibits 5-Å fwhm roughness and the instrument resolution is fixed at $dQ/Q = 0.11$.

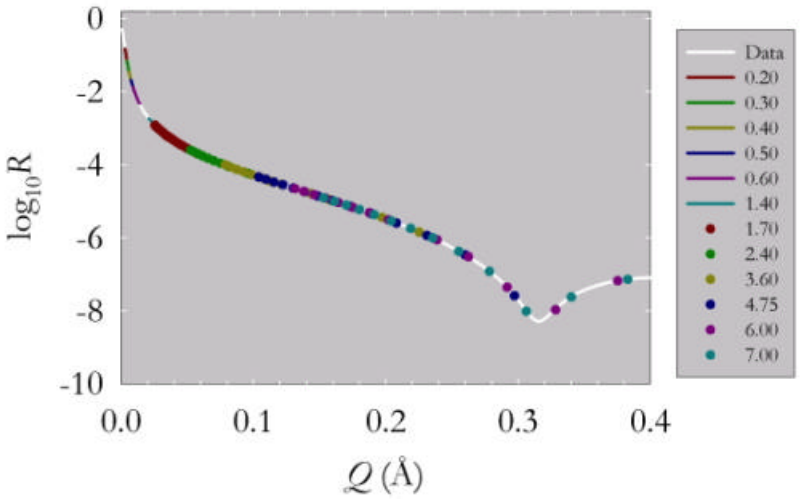

To span the Q range above, we utilized 12 different angles of incidence and employed the bandwidth choppers to select appropriate wavelength bands. The full measurement required 19 different instrument settings. Taking 1000 counts as a reasonable stopping criterion (3% statistics), we can cover the 10^{-8} reflectivity required above in a total counting time of about 2 hours. Most of this time is spent at the largest Q values. If we can achieve 1 count/minute background, then the lowest reflectivity on the above plot can still be measured with a 10:1 signal-to-noise ratio.

For solid samples, one need not scan the incident angular distribution, but can use the tapered-guide centerline position (4.75°) and tip the sample table. Counting times will be shorter.

q (°)	Dl (Å)	t (sec)
0.2	10.5-15	25
0.3	10.5-15	10
0.4	10.5-15	10
0.5	10.5-15	20
0.6	5.5-10	20
	10.5-15	25
1.4	5.5-10	70
	10.5-15	30
1.7	5.5-10	20
	10.5-15	25
2.4	5.5-10	10
3.6	0.5-5	200
	5.5-10	30
4.75	0.5-5	2000
	5.5-10	20
6	0.5-5	2000
	5.5-10	100
7	0.5-5	2000
	5.5-10	100

Possible Improvements

We have proposed a flexible design for a liquids reflectometer that is more than competitive with existing instruments. Overcoming several specific current design constraints would sig-

nificantly improve its performance. All of these involve increasing the bandwidth of the instrument. To whit:

1. One would like more short-wavelength neutrons. The current instrument does not perform very well for $l < 4$ Å. Optimizing the bender and taper segments to reduce this cutoff by even 1 Å would greatly improve counting times and Q coverage.

2. The simulation assumes $4g_c^{Ni}$ guides with 90% average reflectivity will be available in about 2004, not a terribly great stretch from the current state-of the-art….

References

1. J.M. Carpenter and D.F.R. Mildner, Nucl. Instr. And Meth. A **196**, 341 (1982).
2. J.R.D. Copley, J. Neutron Res. **1**, 21 (1993).
3. J.R.D. Copley, Nucl. Instr. And Meth. A **287**, 363 (1990).
4. E.B. Iverson, private communication.